

# An Improved Tungsten-178/Tantalum-178 Generator System for High Volume Clinical Applications

Jeffrey L. Lacy, Mark E. Ball, Mario S. Verani, Henry B. Wiles\*, John W. Babich†, Adrian D. LeBlanc, Michael Stabin, Leonard Bolomey, and Robert Roberts

*Section of Cardiology, Department of Medicine, Baylor College of Medicine, The Methodist Hospital; Johnson Space Center; The Positron Diagnostic and Research Center, The University of Texas Health Science Center, Houston, Texas; and Radiopharmaceutical Internal Dose Information Center, Oak Ridge Associated Universities, Oak Ridge, Tennessee*

Clinical utilization of the multiwire gamma camera (MWGC) requires low-energy radionuclides. The short-lived (9.3 min) tantalum-178 ( $^{178}\text{Ta}$ ) is ideally suited for the MWGC and can be produced from long-lived (21.7 day) tungsten-178 ( $^{178}\text{W}$ ) by a previously reported  $^{178}\text{W}/^{178}\text{Ta}$  generator. This generator, however, is limited by sharp increase in breakthrough after elution of only 30–60 column-volumes. To optimize the  $^{178}\text{W}/^{178}\text{Ta}$  generator for clinical use, varying eluant acid concentrations were evaluated. A reduced (from 0.1 to 0.03N) HCl concentration in the eluant, coupled with low operating temperatures (3 to 5°C) allowed high (40 to 60%)  $^{178}\text{Ta}$  yield. Minimal  $^{178}\text{W}$  breakthrough (<.01%) resulted, even after elution of more than 200 column-volumes. Each of six tested generators provided sterile, high activity (up to 100 mCi)  $^{178}\text{Ta}$  elutions for more than 30 days. Radiation dosimetry was estimated utilizing both human and animal biodistribution data. The whole body (critical organ) dose in adults and neonates were 1/20 (1/21) and 1/19 (1/50) respectively relative to that of technetium-99m ( $^{99\text{m}}\text{Tc}$ ) as sodium pertechnetate. The optimized  $^{178}\text{W}/^{178}\text{Ta}$  generator provides a commercially practical, safe source of low-energy radioisotope for the MWGC with substantial dosimetry advantages over  $^{99\text{m}}\text{Tc}$ .

J Nucl Med 29:1526–1538, 1988

The xenon multiwire gamma camera (MWGC) has many advantages as a nuclear medicine imaging device (1). These include very high count rate, superior resolution, low cost, and favorable hardware characteristics such as compactness, light weight, portability, and ruggedness. Improved imaging performance of the MWGC has been demonstrated and reported elsewhere (2).

One single limitation has precluded realization of so many potential benefits. Practical gaseous detectors have reduced efficiency at the 140-keV energy peak of technetium-99m ( $^{99\text{m}}\text{Tc}$ ). Therefore, isotopes with emission energies well below this level are required. The short-lived tantalum-178 ( $^{178}\text{Ta}$ ) is a candidate with excellent properties. Its emission energy of 55–65 keV

is efficiently detected with moderate gas pressure, and tissue losses relative to  $^{99\text{m}}\text{Tc}$  are modest for most nuclear medicine imaging procedures (1). Furthermore, its short half-life of 9.3 min provides the potential for substantially reduced patient dosimetry relative to  $^{99\text{m}}\text{Tc}$ . Therefore, perfection of a truly practical and economical generator which delivers  $^{178}\text{Ta}$  in large scale for clinical applications represents a significant step in the utilization of the MWGC in nuclear medicine.

We herein report on a  $^{178}\text{W}/^{178}\text{Ta}$  generator optimized for clinical applications, which provides a continuous source of high activity levels of  $^{178}\text{Ta}$  and has a long shelf-life. This system exhibits substantially improved breakthrough and stability over a previously reported system (3–4), by virtue of optimal eluant acid concentration. Most importantly, a low and consistent level of breakthrough is seen over a very large number of elutions in contrast with the previously reported system, which showed rapidly rising breakthrough after only 30–60 elutions. Performance of six high activity

Received July 23, 1987; revision accepted May 5, 1988.

For reprints contact: Jeffrey L. Lacy, PhD, Section of Cardiology, 6535 Fannin, F-905, Houston, TX 77030.

\* Present Address: Medical University of South Carolina, Charleston, SC.

† Present Address: Royal Marsden Hospital, London, England.

units continuously operated in long term clinical studies is reported, together with data on radiation dosimetry of  $^{178}\text{Ta}$  and  $^{178}\text{W}$ . The MWGC imaging results from these clinical studies have been reported elsewhere (2).

## MATERIALS AND METHODS

### Decay Scheme

Tungsten-178 ( $T_{1/2} = 21.7$  days) decays entirely by electron capture to the 9.3 min  $^{178}\text{Ta}$  daughter (5). The short-lived  $^{178}\text{Ta}$  then decays to stable hafnium-178 ( $^{178}\text{Hf}$ ), 99.2% by electron capture and 0.81% by positron emission. Electron capture results in a 61.2% branch to the  $^{178}\text{Hf}$  ground state, 33.7% to the first excited state at 93.1 keV and 4.3% to high-energy Hf levels between 1175 and 1772 keV. Since the 93.1 keV transition is heavily converted, the characteristic x-rays of Hf with energies between 54.6 and 65 keV dominate the  $^{178}\text{Ta}$  emission spectrum. Since  $^{178}\text{W}$  decays exclusively by electron capture to the 9.3 min  $^{178}\text{Ta}$ , it is a pure x-ray emitter. The x-rays and significant gamma ray yields of  $^{178}\text{Ta}$  and  $^{178}\text{W}$  are tabulated in Table 1 (5).

### Production and Purification of $^{178}\text{W}$

The  $^{178}\text{W}$  parent isotope was produced by the p,4n reaction on natural  $^{181}\text{Ta}$ . Cyclotron irradiations were performed in an external cyclotron beam utilizing a solid target of 1-mm thickness. The following parameters were typical of these runs:

Proton energy: 40 MeV;

Operating current: 60  $\mu\text{A}$ ;

Production rate at EOB: 0.7 mCi/ $\mu\text{A}\cdot\text{hr}$  (26 MBq/ $\mu\text{A}\cdot\text{hr}$ );

Typical yield: 42 mCi/hr (1.55 GBq/hr);

Irradiated target area: 1.27 cm diameter (2 g).

The 40-MeV beam loses 13 MeV in the 1-mm target; thus, the production energy range from front to back of the target is 40 to 27 MeV. The proton Ta production cross-sections have been previously reported (6). The p,4n reaction cross-section peaks in the middle of this energy range. The only

significant competing reactions are p,3n and p,5n which produce  $^{179}\text{W}$  and  $^{177}\text{W}$ , respectively. In the center of the production energy range these reaction cross sections are less than one-tenth of p,4n. However, the p,3n reaction becomes significant at 27 MeV and the p,5n reaction at 40 MeV. These  $^{179}\text{W}$  and  $^{177}\text{W}$  isotopes decay by electron capture with half-lives of 37.5 min and 2.25 hr, respectively, to long-lived Ta species  $^{179}\text{Ta}$  ( $T_{1/2} = 655$  days) and  $^{177}\text{Ta}$  ( $T_{1/2} = 56.6$  hr), which in turn decay to stable  $^{179}\text{Hf}$  and  $^{177}\text{Hf}$ . Since chromatographic separation of W from both Ta and Hf is performed to purify  $^{178}\text{W}$ , the potential contaminants can be conveniently eliminated by assuring decay of  $^{177}\text{W}$  and  $^{179}\text{W}$  before processing. A 2-day delay between irradiation and processing leads to 6% loss of  $^{178}\text{W}$  while decaying the  $^{179}\text{W}$  and  $^{177}\text{W}$  by 77 and 21 half-lives, respectively. Such decay is also advantageous to reduce shielding requirements during processing.

After such decay, only Ta and Hf contaminant species are present. Separation of  $^{178}\text{W}$  from the 2-g target is achieved by a previously described method which provides highly selective chromatographic separation of W from both Ta and Hf (6). The process produces a  $^{178}\text{W}$  solution in 0.1N HCl and 1%  $\text{H}_2\text{O}_2$  with a volume of 2 ml which is directly loaded onto the generator column.

### Column Design and Preparation

The generator column utilizes the anion exchange resin AG 1-X8 (Bio-Rad, Richmond, CA) in chloride form (200–400 mesh). This resin is highly stable and can be autoclaved in aqueous media at 120°C (7). A schematic of the generator column is shown in Figure 1. A borosilicate glass barrel is employed (0.5 cm  $\times$  7.6 cm, volume = 1.5 ml). The anion exchange resin is contained within this column by 30  $\mu\text{m}$  porosity polyethylene frits which are sealed to the end of the column with a teflon collar having a small diameter (0.55 mm) output port. Input/output connections are made with standard high performance liquid chromatography (HPLC) teflon tubing (0.5 mm inner diameter (ID)) and connectors.

The column is prepared as follows. The AG 1-X8 resin is equilibrated in 0.03N HCl, 0.1%  $\text{H}_2\text{O}_2$  and loaded into the column. The sealed column, including attached plumbing, is then autoclaved at 120°C for 15 min and flushed with 30 ml of sterile eluant. The 2-ml (0.1N HCl, 1%  $\text{H}_2\text{O}_2$ )  $^{178}\text{W}$  solution resulting from the target separation process is then aseptically loaded and the column immediately flushed with 30 ml of eluant (0.03N HCl, 0.1%  $\text{H}_2\text{O}_2$ ). The generator is then ready for use.

A schematic of the overall system is shown in Figure 2. The generator column, 500 ml eluant reservoir, and connection tubing are integrated within a small portable refrigeration unit. This unit is run at 3 to 5°C during operation of the system to facilitate significantly increased  $^{178}\text{Ta}$  yield. The refrigeration unit also serves as a convenient protective housing. Only the elution supply syringe and output port, connected to the column output by 30 cm of 0.5 mm ID teflon HPLC tubing terminated with a female Luer fitting, are accessible externally.

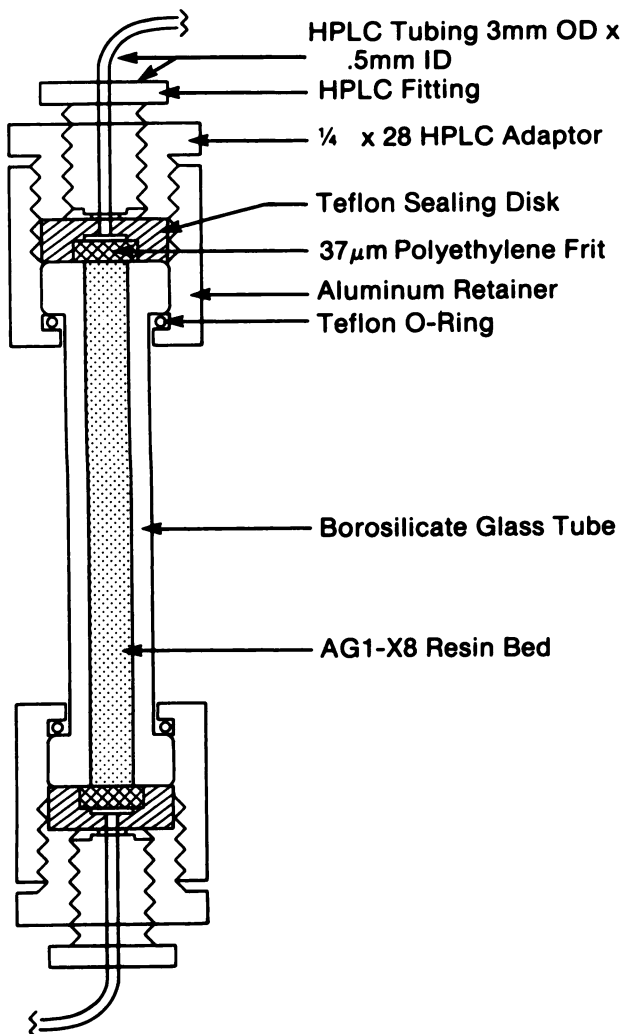
Elution of the system is accomplished very simply and quickly. A 3-ml syringe is loaded with 0.5 ml disodium phosphate ( $\text{Na}_2\text{HPO}_4$ ) buffer solution required to adjust the eluate (pH 1.8) to pH 7.0, fitted with disposable 0.22- $\mu\text{m}$  filter and attached to the generator output port. A volume of 1.5 ml of eluant is drawn up into the supply syringe and imme-

TABLE 1  
 $^{178}\text{Ta}$  and  $^{178}\text{W}$  Emissions

| $^{178}\text{Ta}$ (9.3 min $T_{1/2}$ )<br>emission by energy | Intensity<br>(%) | Mean energy<br>(keV) |
|--|------------------|----------------------|
| K alpha x-ray  | 67.4             | 55                   |
| K beta x-ray   | 17.7             | 64                   |
| Gamma 1  | 6.5              | 93                   |
| Gamma 5  | 0.1              | 213                  |
| Gamma 11 + 12  | 0.1              | 998                  |
| Gamma 13 + 14  | 0.5              | 1108                 |
| Gamma 15–22  | 0.3              | 1224                 |
| Gamma 23 + 24  | 2.2              | 1346                 |
| Gamma 25   | 0.5              | 1403                 |
| Gamma 29–33  | 0.3              | 1497                 |

| $^{178}\text{W}$ (21.7 days $T_{1/2}$ )<br>emission by energy | Intensity<br>(%) | Mean energy<br>(keV) |
|---|------------------|----------------------|
| K alpha x-ray   | 17.1             | 57                   |
| K beta x-ray  | 4.5              | 66                   |



**FIGURE 1**  
 $^{178}\text{W}/^{178}\text{Ta}$  generator column schematic. HPLC = high performance liquid chromatography.

diately pushed through the column. The check valve assembly (Burrton Medical Inc., Bethlehem, PA) MAT-4100 serves to route eluant from the supply bottle to the elution syringe and thence to the generator during elution. The system remains totally sealed throughout clinical use. A sterile plug or syringe is installed at the output port at all times to prevent microbial contamination.

#### Test Generators

In order to overcome the limited elution capacity and precipitous onset of breakthrough demonstrated by the previously reported generator, we tested columns employing reduced HCl concentration ranging from 0.1N to 0.03N (4). A total of 15 test generators utilizing 50  $\mu\text{Ci}$  to 50 mCi  $^{178}\text{W}$  activity were constructed and evaluated to determine yield, breakthrough, elution profile, temperature performance, and consistency of operation. All of these units had 1.5 ml volume and were similar in configuration to that described above. They were typically eluted at 1 hr intervals to provide asymptotic buildup of  $^{178}\text{Ta}$ . Breakthrough levels were measured at least 2.5 hr post-elution to assure full decay of  $^{178}\text{Ta}$ . Both breakthrough and yield measurements were performed by

counting the samples over a multiwire proportional detector (25 cm diameter) relative to a  $^{178}\text{W}$  calibration standard. In this technique, only the  $^{178}\text{W}$  and  $^{178}\text{Ta}$  x-rays are detected by the thin gaseous detector which has a very low sensitivity for gamma rays above 100 keV. An appropriate correction for x-ray yield differences was utilized to determine the calibration factor for  $^{178}\text{W}$  in equilibrium with  $^{178}\text{Ta}$  and for that of pure  $^{178}\text{Ta}$ . From Table 1 the x-ray yield of  $^{178}\text{W}$  is 21.6% while that of  $^{178}\text{Ta}$  is 106.7%. Thus, the x-ray yield of equilibrium  $^{178}\text{W}/^{178}\text{Ta}$  is 1.25 times that of pure  $^{178}\text{Ta}$ . An online computer (LSI 11/23) was utilized to perform automated decay correction and calibration scaling.

Elution profile was measured by rapid elution of 0.1-ml samples onto successive locations along an absorbent paper strip. Isolated active areas were then clipped from the strip and assayed over the area multiwire proportional counter detector with decay correction. This procedure allowed very rapid (15 to 20 sec) elution, eliminating regenerated activity in the profile. All breakthrough and yield measurements, unless otherwise stated, are quoted as a percent of the total  $^{178}\text{W}$  loaded on the column, which is also the maximum theoretic yield of  $^{178}\text{Ta}$ . All yield measurements were based upon elutions after a minimum 45 min regeneration time unless otherwise specified.

Columns tested during periods of elevated laboratory temperature (on weekends and evenings, when air conditioning was turned off), exhibited a significant depression of yield from 28% down to 10%, as the laboratory temperature increased from 24° to over 30°C. Subsequently, dependence of generator performance on temperature was assessed using a temperature controlled water bath with temperatures ranging from 4° to 24°C.

An HCl concentration of 0.03N was chosen as a good compromise providing greatly increased total elution capacity with only slightly reduced yield when operated at a column temperature of 3 to 5°C. Long-term performance and stability was then evaluated over 30 days utilizing this concentration. For this study, each unit functioned through temperatures ranging from 4 to 24°C during the extended test period. Several daily measurements of both yield and breakthrough were performed and are reported as percent of total  $^{178}\text{W}$  on the column.

Generator yield versus buildup time was determined for 0.03N HCl at 24° and 4°C. Elutions were performed at 0.5, 1, 2, 4, 8, 9.3, 18.6, 27.9, and 45.0 min, assayed and decay-corrected to the elution time. Yield as a percent of  $^{178}\text{Ta}$  made available by  $^{178}\text{W}$  decay during the buildup interval was calculated at each point.

#### Clinical Generators

Each of six large generators with  $^{178}\text{W}$  activity ranging from 57 to 158 mCi (mean  $\pm$  SD 98  $\pm$  32 mCi) were utilized on a continuous basis for clinical evaluation of first-pass ventriculography with the MWGC. Each unit provided a full 30 days of clinical use and in addition, each unit was extended 30 days on a test basis while a newer unit provided clinical activity. All of these generators were operated at 3 to 5°C throughout the test period.

To document performance, test elutions were obtained prior to use in the morning and at the end of each day. Such samples were assessed for breakthrough after 2.5 hr of decay of the  $^{178}\text{Ta}$  activity. The previous afternoon sample was

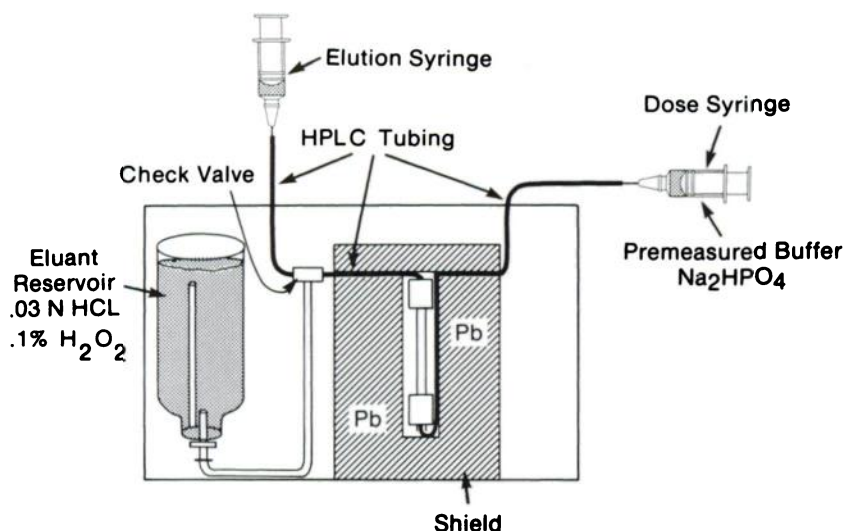


**FIGURE 2**  
Clinical  $^{178}\text{W}/^{178}\text{Ta}$  generator schematic. HPLC = high performance liquid chromatography.

assessed each morning by measurement in a standard dose calibrator with appropriate calibration factor. This provided daily assessment of breakthrough. A breakthrough level of 10  $\mu\text{Ci}$  was set as the upper limit for patient injection. The twice-daily samples were kept and counted weekly in a sodium iodide (NaI) well counter for more accurate determination of breakthrough. The yield of each elution was measured in the laboratory dose calibrator with appropriate correction factor established by comparison with NaI well counter measurements. The half-life of the  $^{178}\text{Ta}$  is long enough to allow such measurement prior to patient injection, without significant loss of activity.

#### Biologic and Chemical Purity

A pyrogenicity test was completed on each generator prior to clinical use either by the limulus lysate procedure or by the rabbit temperature rise method. Cultures for both aerobic and anaerobic bacteria as well as fungus were immediately begun on initial eluate samples of all generators and were repeated at 30 days on selected units to verify initial and long-term aseptic performance. For all sterility tests, samples were taken without the 0.22- $\mu\text{m}$  filter installed.

Tungsten and tantalum metal levels were measured in selected eluate samples by mass spectroscopy. The samples were collected randomly from the six clinical generators with a regeneration time of 45–60 min. Radioisotopic purity of the loading solution was assured through Ge(Li) spectroscopy.

#### Animal Biodistribution Studies

Biodistribution of  $^{178}\text{W}$  breakthrough was studied in ten infant (8 to 9 days) and nine adult Sprague-Dawley rats. The rats were injected with phosphate buffered generator eluate containing 8 to 10  $\mu\text{Ci}$  of  $^{178}\text{W}$ . Adult animals received injections in the tail vein, while infants received intracardiac injections. Intracardiac injection was necessary in the infants because superficial veins were not available for consistently successful cannulation. All infants survived this procedure and recovered without any observable ill effects. Organ retention was determined at 0.5, 2, 8, 24, and 48 hr by counting in a NaI well counter. Organ wet weights were recorded immediately after dissection. Percent in animal organs was converted to percent in human organs by multiplying by the ratio

of the organs fraction of total body weight in the human to that in the animal. Human organ weights were derived from MIRSD Pamphlet No. 5, revised (8) and Cristy and Eckerman's report on the pediatric phantoms (9) for the adult and newborn, respectively.

#### Human Biodistribution Studies

The whole-body excretion curve of  $^{178}\text{W}$  breakthrough was determined in six human subjects. These subjects were injected with 2  $\mu\text{Ci}$  of  $^{178}\text{W}$  as phosphate buffered eluate and then counted in a whole-body counter (NASA-Johnson Space Center, Houston, TX) immediately after injection and at regular intervals thereafter for 14 days.

Time dependence of the labeling of the human blood pool with directly injected phosphate buffered  $^{178}\text{Ta}$  was determined by drawing blood samples from seven subjects at 2 min, 5 min, and every 5 min thereafter to 25 min after injection with 20 to 45 mCi  $^{178}\text{Ta}$ . The data for each subject, beginning at the 5 min sample to assure thorough mixing, were fit to a single exponential and normalized to 100% at  $T = 0$  utilizing extrapolation of this exponential fit. Using blood volume estimated by body surface area, absolute blood retention was calculated to rule out heavy extravasation during first transit.

Brief static images over the full extent of the subject torso were obtained in five of the subjects immediately after completion of the first-pass radionuclide angiography data acquisition, as well as at 15 and 30 min later. These images were qualitatively assessed for any possible specific organ uptake.

#### Human Radiation Dose Estimates

Regression analyses of percent uptake per organ values for  $^{178}\text{W}$  obtained from adult and pediatric rats provided initial uptake fractions and clearance half-times for human adults and newborns. Activity not accounted for was considered to be uniformly distributed in the remainder of the body. The human data for whole-body retention were used to define the clearance half times for this activity. These human data were considered to be more reliable predictors for both adult humans and neonates than animal whole body data due to the substantial species differences exhibited.

Dose estimates for  $^{178}\text{Ta}$  are based on the assumption that

the activity is uniformly distributed in the blood pool and eliminated through the urine. This model is supported by spot imaging in subjects injected with  $^{178}\text{Ta}$  which are consistent with pure intravascular and bladder distribution up to 30 min postinjection. Animal studies were not deemed valid for this study since early measurements by ourselves and others in both dogs and rats showed much more rapid extravasation than in humans (10-11). The retention half-time determined from the blood samples taken from human subjects was used to define these kinetics. The S-value for the blood for  $^{178}\text{Ta}$  was derived from the S-value for the whole body, but assuming a target mass of 5,400 g (12) and assuming that all electron energy is absorbed within the blood.

Calculations were performed using the standard MIRD schema (13) with S-values derived for standard man (8) and Cristy and Eckerman's newborn phantom (9). The dynamic bladder model of Cloutier et al. (14) and the excess cumulated activity correction (15) were employed. Bladder voiding intervals of 1.0 and 4.8 hr were used for the newborn and adult, respectively.

## RESULTS

### Test Generators

The dependence of  $^{178}\text{Ta}$  yield upon HCl concentration ranging from 0.03 to 0.1N is shown in Table 2 for room temperature (24°C) and 4°C operation. Yield is seen to increase with increasing HCl concentration at both 24 and 4°C. However, at 4°C, significantly increased yield is seen for all HCl levels allowing operation at much lower HCl levels while maintaining reasonable  $^{178}\text{Ta}$  yield.

Generator elution profiles measured at 0.03 and 0.1N HCl for 4° and 24°C operation are shown in Figure 3. No significant difference in shape is seen in these profiles indicating that the molecular form of  $^{178}\text{Ta}$  is very likely not altered by HCl concentration or temperature. Activity is highly mobile with initial appearance corresponding approximately to the void volume of the column and output plumbing (0.3 ml). Near total activity delivery is achieved in a volume of 0.5 ml or 0.33 column volumes.

A typical 30-day performance test with 0.03N HCl is shown in Figure 4 for a generator loaded with 50 mCi  $^{178}\text{W}$ . Multiple daily yield and breakthrough measurements were performed. The total eluted volume was 230 ml or more than 150 column volumes. The unit was cycled through the temperature range 4-24°C several times during the test period. The depressed yield during the increased temperature periods can be noted. The yield on Day 0 varied from 49% at 4°C to 22% at 24°C. At 30 days, the yield decreased to 36% at 4°C and 14% at 24°C. Smooth breakthrough behavior was exhibited as a function of eluted volume with a minimum breakthrough occurring at ~150 ml followed by a very gradual rise. The mean breakthrough level over 30 days and 150 column volumes was  $0.0012 \pm 0.00072\%$ . The breakthrough shows some dependence

**TABLE 2**  
 $^{178}\text{Ta}$  Yield as a Percent of Maximum Theoretical Yield Versus HCl Normality at 4 and 24°C\*

| HCL [N] | 4°C | 24°C |
|---------|-----|------|
| 0.03    | 57  | 28   |
| 0.05    | 69  |      |
| 0.10    | 90  |      |
| 0.15    |     | 54*  |

\* All measurements were made with asymptotically long buildup time (>1 hr).

† Neirinckx RD, Trumper J, LeBlanc A, Johnson PC. Radio-nuclide generators. Evaluation of adsorbents for the Ta-178 generator. ACS Symposium Series 1983; 151-167.

upon the time elapsed since the previous elution with higher values corresponding to greater than 12 hr buildup and lower values to less than one hour buildup. No increase is seen over the 12-hr level even after several days demonstrating that the process is self-limiting.

The  $^{178}\text{Ta}$  yield as a percentage of  $^{178}\text{Ta}$  made available by  $^{178}\text{W}$  decay is shown in Figure 5 for 4°C and 24°C operation versus the time since previous elution. A substantially lower yield is seen at 24°C for long regeneration intervals, but a sharp increase in yield is seen at short regeneration intervals so that yields are nearly equal at 0.5 min independent of temperature. Thus the primary beneficial effect of lowered temperature clearly lies in preservation of mobility of  $^{178}\text{Ta}$  produced by  $^{178}\text{W}$  decay which occurred several minutes or more prior to elution. In Figure 6 the generator yield buildup at 4°C and 24°C is shown relative to the ideal buildup predicted assuming that all  $^{178}\text{Ta}$  made available by physical decay is eluted. The buildup curve for 24°C is seen to be much more rapid than the theoretic curve when expressed as a percent of the maximum observed yield for long buildup time. The 4°C data, on the other hand, lies only slightly above the theoretic curve despite the fact that the absolute yield at long regeneration intervals is far from 100%.

### Clinical Generator Yield and Breakthrough Performance

The results of yield and breakthrough measurements on six clinical generators ranging in  $^{178}\text{W}$  activity from 57 to 158 mCi are shown in Figures 7 and 8. Since yield was found to be primarily affected by shelf-life and not dependent on eluted volume, it is plotted against days of use. Breakthrough, on the other hand, is dependent on eluted volume and is thus plotted versus this variable. Both yield and breakthrough are corrected for  $^{178}\text{W}$  decay. In every case, the performance was evaluated under realistic circumstances of frequent repeated elution over a lengthy period. Yield is seen to decrease somewhat with shelf life. This fall off is most rapid during the first 20 days, decreasing at a rate of ~0.5% per day. The falloff rate decreases substantially to about 0.1% per day in the interval from 40 to 60

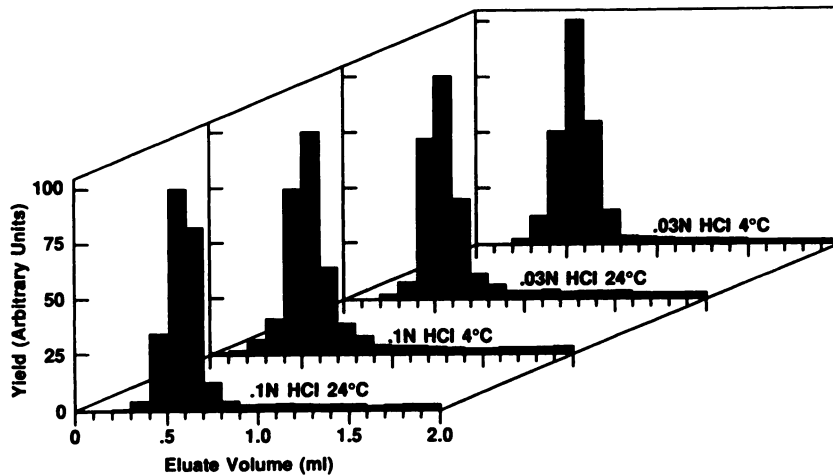


**FIGURE 3**  
Elution profiles at 4 and 24°C for 0.03N and 0.1N HCl.

days. The mean yield on Day 3 was 57% and at Day 30 was 40%. Breakthrough is seen to decrease over the first 120 ml of eluted volume and then flattens out until ~250 ml at which point a very slow rise is shown up to 300 ml. Breakthrough performance is seen to be less than 0.0014% up to 300 ml.

#### Biologic and Chemical Purity

All generators had negative pyrogen tests prior to clinical use. Cultures of eluate samples from the first and thirtieth day of clinical use from all units were negative demonstrating consistent preservation of sterility. No adverse reactions were observed in 61 patients injected with buffered  $^{178}\text{Ta}$  eluate.

Tantalum metal levels in the eluate ranged from undetectable levels (<5 parts per billion) to 330 parts per billion ( $3.3 \times 10^{-7}\text{g/injection}$ ). Tungsten metal levels were all below the detectable limit of 5 parts per billion. No radioisotopic contaminants were detected with Ge(Li) spectroscopy.

#### Human Biodistribution Estimates

Results of  $^{178}\text{Ta}$  blood activity measurements in adult humans are shown in Figure 9. The data are well represented by a single exponential function with a half-time for blood retention of 87.5 min. The blood-pool labeling efficiency (mean  $\pm$  s.d.) at 25 min is  $82.7 \pm 7.9\%$ . Torso static images of  $^{178}\text{Ta}$  were consistent with near total blood-pool activity distribution, indicating no substantial organ uptake other than slight bladder activity at 30 min. This treatment does not rule out the possibility of anomalous losses of activity during the first transit through the circulatory system. However, direct computation of the absolute blood activity at 5 min, employing an estimated blood volume of 71.4 ml per kg of body weight, yields a labeling efficiency of  $88.0 \pm 12.7\%$ , consistent with the value of  $96.1 \pm 1.5\%$  obtained by exponential extrapolation. Thus, a single excretion route via the urine is assumed to be a good approximation for radiation dose estimates.

Whole-body retention of  $^{178}\text{W}$  is shown in Figure 10. Whole-body activity measurements in six subjects are

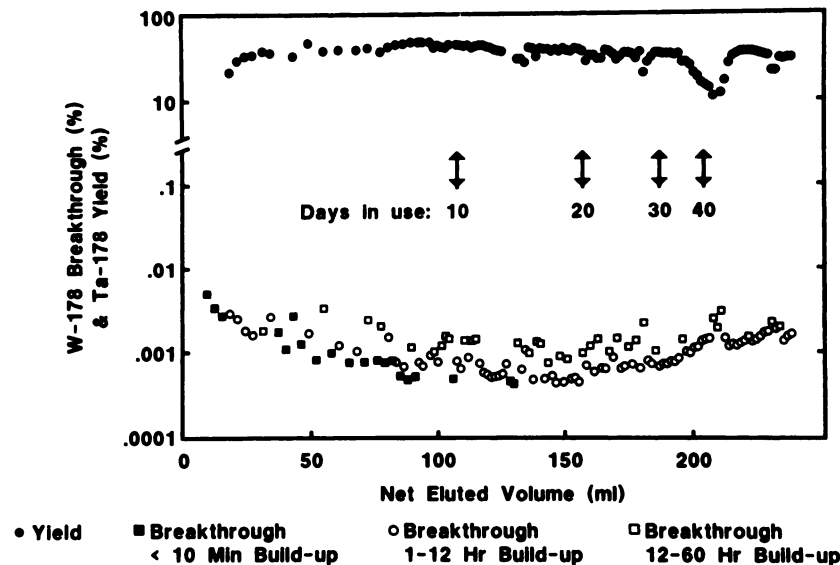


**FIGURE 4**  
Yield and breakthrough performance of 0.03N HCl, 0.1%  $\text{H}_2\text{O}_2$  generator over a 41-day period.

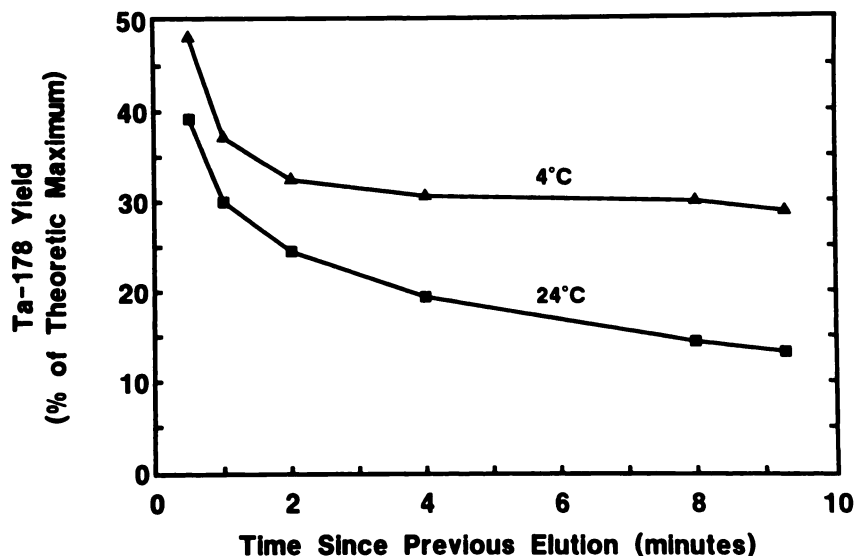


**FIGURE 5**  
 $^{178}\text{Ta}$  yield as percent of theoretic maximum for short regeneration times at 4 and 24°C.

plotted over a 20-day period. The excretion curve is well represented by three exponential components with 94.5% excretion with a half-time  $T_b = 8$  hr, 4% with  $T_b = 35$  hr, and 1.5% with  $T_b = 11$  days.

Organ retention for the adult and pediatric rat is reported in Table 3. Table 4 lists the results for initial uptakes and double exponential clearance half-times for  $^{178}\text{W}$  estimated for various organs of the human, based on the extrapolation of the animal data of Table 3. Also shown are the whole body retention biologic half-times derived from triple exponential fits to the human whole-body counting measurements for  $^{178}\text{W}$  and utilized for washout of the remainder of the activity not accounted for by organ data. The table also shows the single exponential model used to describe the  $^{178}\text{Ta}$  kinetics, based on the human blood counting data (1.46 hour half-time).

#### Radiation Dose Estimates

Absorbed dose estimates for human adults and newborns calculated according to the MIRD guidelines are shown in Tables 5 and 6 respectively. The dosimetry of phosphate buffered  $^{178}\text{Ta}$  eluate is compared with  $^{99\text{m}}\text{Tc}$  as sodium pertechnetate. Absorbed dose estimates for sodium pertechnetate were derived using the kinetic model of MIRD Dose Estimate Report No. 8 (16) with the phantoms for standard man (8) and Cristy and Eckerman's newborn phantom (9). In the adult, the organ receiving the highest absorbed dose is the bladder for both  $^{178}\text{W}$  and  $^{178}\text{Ta}$ . A shorter bladder voiding interval will reduce the bladder wall dose and, to a lesser extent, the gonadal doses. For the newborn, the skeleton receives the highest dose from  $^{178}\text{W}$ , followed by bladder wall and red marrow. The bladder wall receives the

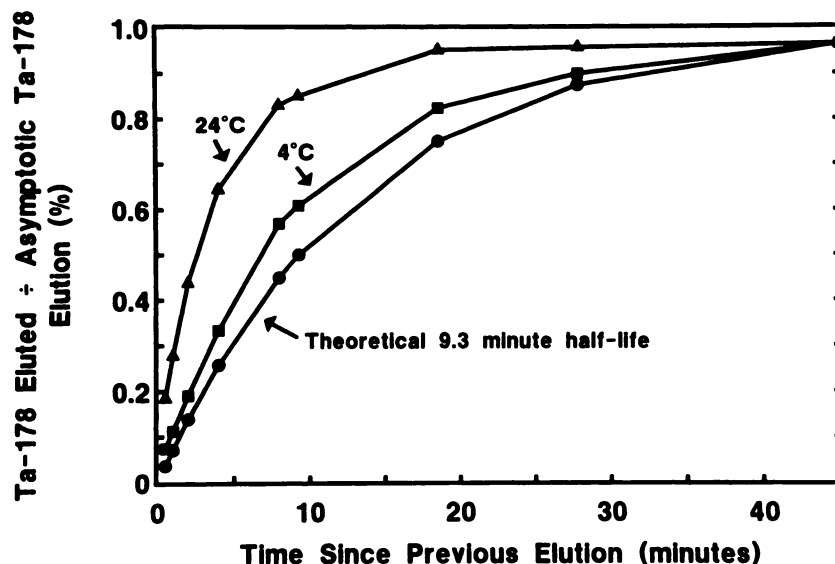


**FIGURE 6**  
 $^{178}\text{Ta}$  yield as percent of the maximum observed yield for long buildup times (asymptotic yield) at 4 and 24°C compared with theoretical regeneration by physical decay (9.3-min half-life).

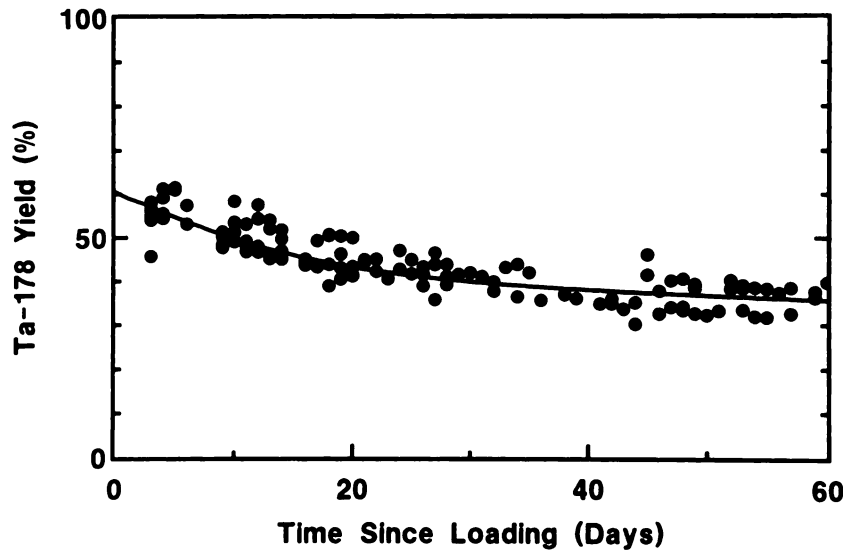


**FIGURE 7**  
Composite yield performance of six clinical generators evaluated over 60 days of use.

highest dose from  $^{178}\text{Ta}$  for the newborn. In the infant, less control over bladder voiding interval is possible. Keeping the individual well hydrated will keep the bladder volume high and the radioactivity concentrations low. The low breakthrough of  $^{178}\text{W}$  from this generator system of  $<0.1 \mu\text{Ci}$  per mCi of injected  $^{178}\text{Ta}$  reduces the influence of  $^{178}\text{W}$  to a very low level relative to the  $^{178}\text{Ta}$  dose.

## DISCUSSION

### Generator Performance

The narrow elution profile measurements indicate that a single charge species of the  $^{178}\text{Ta}$  compound is present. This compound is highly mobile over a wide range of temperature and HCl concentration. In contrast to our measurements, Neirinckx et al. (3) observed a significant tailing of the profile after one column volume and speculated on the existence of multiple charge species. A probable explanation for this discrepancy

is regeneration during the extended elution time required for the large elution volumes used by Neirinckx (9 ml total column volume). In our measurements, all elution samples were obtained in  $<20$  seconds, thus minimizing the effects of regeneration during the collection period.

In view of the consistency of  $^{178}\text{Ta}$  mobility as represented by the elution profile versus both temperature and HCl concentration, it is likely that a highly mobile Ta species is formed upon decay of the  $^{178}\text{W}$  but that this compound in the environment of the column has a limited chemical lifetime which is substantially increased by higher HCl concentration and lowered temperature. This hypothesis is supported by the observation that even at high temperature and low HCl concentrations a high percentage of  $^{178}\text{Ta}$  made available by decay is eluted from the column for very brief regeneration intervals. The agreement of the regeneration curve at  $4^\circ\text{C}$  with ideal buildup by physical decay and the fact that even at 0.5 min buildup, only  $\sim 50\%$

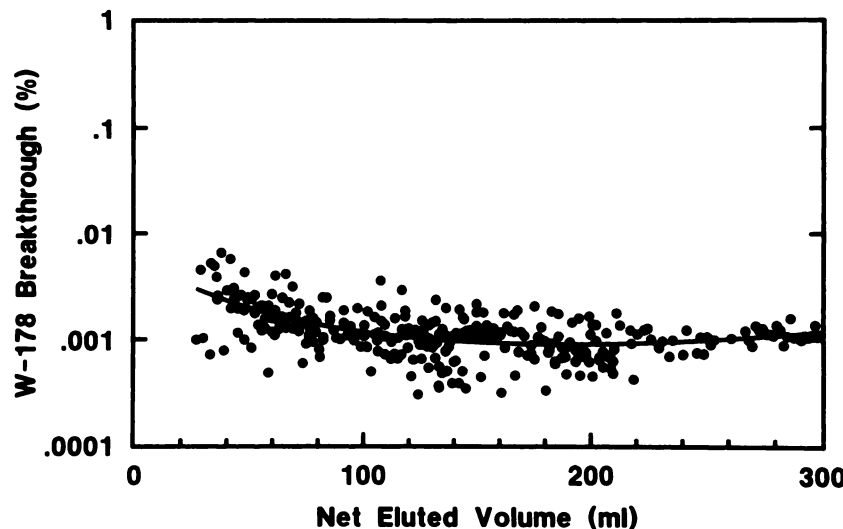


**FIGURE 8**  
Composite breakthrough performance of six clinical generators evaluated up to 300 ml total eluted volume.

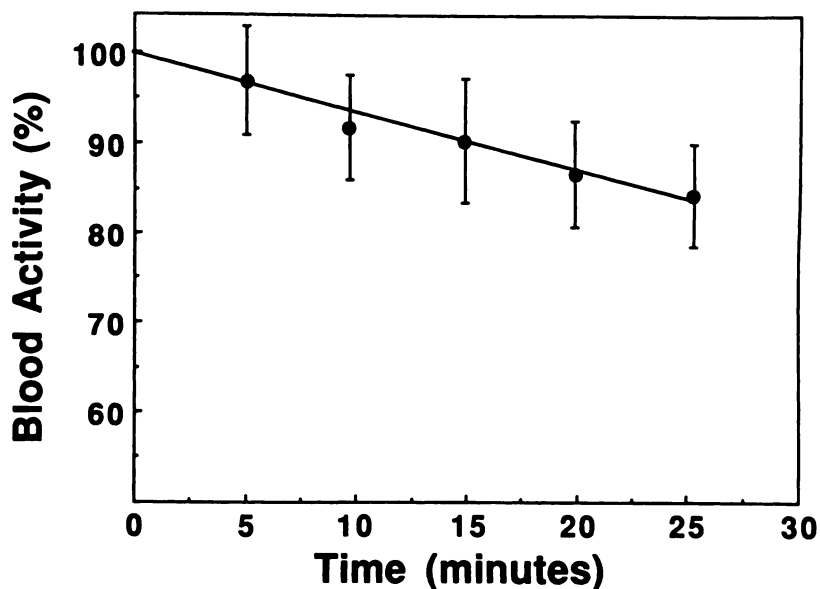


**FIGURE 9**  
Blood retention of phosphate-buffered  $^{178}\text{Ta}$  in seven adult human subjects.

of available activity is eluted, suggests that a rapid loss mechanism with a half-time much  $<1$  min is operative for some fraction of the  $^{178}\text{W}$  decay. The remaining fraction for 0.03N HCl is likely lost to chemical decomposition at a rate which is heavily dependent upon temperature. It would appear that all or most of this component is preserved when the column is operated at  $4^\circ\text{C}$ . Earlier work speculated that the  $^{178}\text{Ta}$  mobility was modified by HCl concentration (3). This is clearly contradicted by our measurements.

Utilization of 0.03N HCl provides a very substantial improvement in total elution capacity relative to 0.1N HCl. Good performance is achieved to at least 200 column volumes. Perhaps most importantly, with the low level of HCl, rapidly rising breakthrough is never observed. Thus, breakthrough performance can be easily monitored during clinical use with daily performance well represented by the previous day's measurement. Although eluant yield is substantially reduced by

lowered HCl this effect is minimized by operation near  $0^\circ\text{C}$ . Thus, only a small price is paid for the very important improvement in safety provided by the use of lower HCl concentration.

A 1-ml elution (0.67 column volumes) is more than adequate to remove all available activity. Thus, the volume of 1.5 ml utilized in this work can be reduced to 1.0 ml yielding substantially more elutions before any breakthrough rise occurs. This smaller injected volume is preferable for a compact first pass bolus. If smaller injected volumes are required for pediatric patients, the generator column volume could be reduced substantially with little effect expected on yield or breakthrough performance since the  $^{178}\text{W}$  is prepared in tracer-free form. Radiation dose to the resin becomes more significant at very small resin volumes. However, there was no indication of such effects as the  $^{178}\text{W}$  activity was varied over a very wide range in this study of 0.1 to 200 mCi.

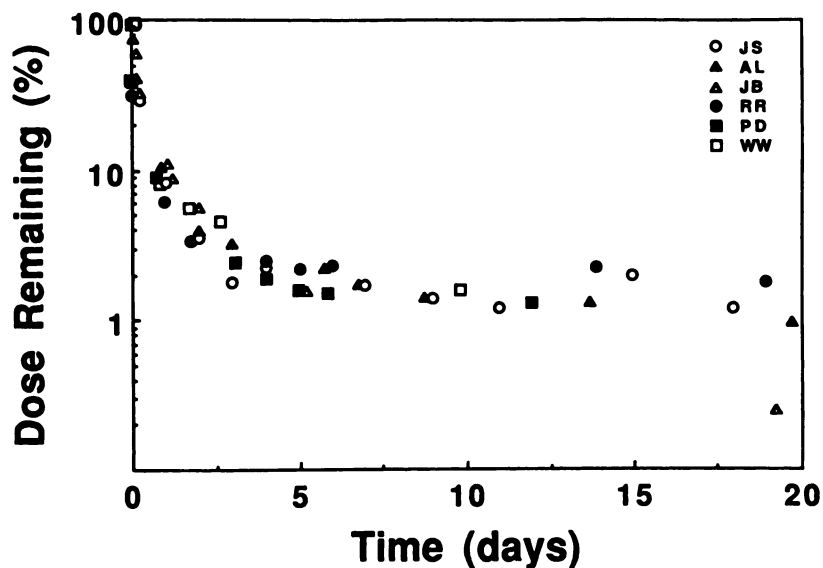


**FIGURE 10**  
Whole-body retention of phosphate-buffered  $^{178}\text{W}$  in six adult human subjects.

**TABLE 3**  
Organ Retention of <sup>178</sup>W Expressed as Mean% Uptake Per Gram of Tissue in Adult and Pediatric Rats

| Organ           | Adult                   |      |       |       |        |
|-----------------|-------------------------|------|-------|-------|--------|
|                 | Time Postinjection (hr) |      |       |       |        |
|                 | 0.5                     | 2    | 8     | 24    | 48     |
| Heart wall      | 0.23                    | 0.09 | 0.007 | 0.003 | 0.0015 |
| Small intestine | 0.51                    | 0.48 | 0.07  | 0.04  | 0.015  |
| Large intestine | 0.11                    | 0.12 | 0.38  | 0.26  | 0.12   |
| Kidney          | 1.63                    | 1.06 | 0.35  | 0.24  | 0.11   |
| Liver           | 0.55                    | 0.25 | 0.03  | 0.02  | 0.02   |
| Lung            | 0.34                    | 0.12 | 0.01  | 0.008 | 0.007  |
| Skeleton        | 1.07                    | 0.75 | 0.35  | 0.21  | 0.18   |
| Spleen          | 0.29                    | 0.12 | 0.05  | 0.04  | 0.04   |

| Organ      | Pediatric               |       |      |      |      |
|------------|-------------------------|-------|------|------|------|
|            | Time Postinjection (hr) |       |      |      |      |
|            | 0.5                     | 2     | 8    | 24   | 48   |
| Brain      | 1.6                     | 0.83  | 0.30 | 0.13 | 0.04 |
| Heart wall | 2.98                    | 1.32  | 0.34 | 0.16 | 0.22 |
| Kidney     | 7.34                    | 3.58  | 1.52 | 0.97 | 0.29 |
| Liver      | 5.65                    | 3.77  | 1.40 | 0.69 | 0.21 |
| Lung       | 3.18                    | 1.54  | 0.47 | 0.33 | 0.14 |
| Skeleton   | 10.21                   | 10.79 | 8.73 | 6.54 | 3.84 |
| Spleen     | 3.24                    | 0.89  | 0.92 | 0.68 | 0.29 |

### Biologic and Chemical Purity

All generators of this study performed with complete safety with regard to toxicity and sterility. The measurable Ta metal levels are extremely small compared with the LD50 for tantalum chloride measured in the rat of 38 mg/kg (17). The maximum observed tantalum level of  $3.3 \times 10^{-7}$  g/injection is  $1.2 \times 10^{-8}$  of LD50.

A thorough assessment of organic contaminants was previously carried out on an AG 1-X8 <sup>178</sup>W/<sup>178</sup>Ta generator eluted with 0.15N HCl eluant (4). The only compound present was trimethylamine. It was concluded that this compound is produced through breakdown of the resin by the acidic eluant as no change in level was seen when high activity generators were compared with ones containing no activity at all. Levels ranging from 2 ppm to 9 ppm were seen for buildup times ranging from 1 day to 38 days. The LD50 level of trimethylamine in the mouse is 90 mg/kg (18). Injection of 1.5 ml of eluant in a 70-kg patient therefore provides a dose of no more than  $1.9 \times 10^{-4}$  mg/kg which is  $2 \times 10^{-6}$  of LD50 assuming a buildup time of 38 days. In typical clinical use buildup times of no more than 1 day should be seen. Therefore the very low levels of nonradiolytic organic contaminant are of no significant concern.

The system is carrier-free and requires no flushing of contaminant radioisotopes, as for example is required with the <sup>195m</sup>Hg/<sup>195m</sup>Au generator, making it inherently safe both with regard to chemical contaminants and

**TABLE 4**  
Estimated Human Organ Uptake of <sup>178</sup>W Based on Percent Injected Activity Uptake in the Rat Scaled by the Ratio of the Organs Fraction of Total-Body Weight in the Human to that in the Animal\*

|            | Percent uptake | Biologic half-lives/in hr from double exponential fit |                           |
|------------|----------------|---|---------------------------|
| Adult†     |                | Exponential 1<br>[HR (%)]                             | Exponential 2<br>[HR (%)] |
| Heart Wall | 0.24           | 1.4 (98.9%)   | 55 (1.1%)                 |
| Kidney     | 1.6            | 2.7 (84%)   | 44 (16%)                  |
| Liver      | 3.5            | 1.4 (97.2%)   | ∞ (2.8%)                  |
| Lung       | 1.4            | 1.05 (96.4%)  | 28 (3.6%)                 |
| Bone       | 18.4           | 2.2 (77%)   | 79 (23%)                  |
| Spleen     | 0.22           | 0.94 (88%)  | 55 (12%)                  |
| Remainder‡ | 71.6           | 8.1 (94.5%)   | 37.5 (4.0%)               |
|            |                |   | 535 (1.5%)†               |

3% assumed to be taken up by small intestine and excreted via normal GI kinetics.

| Newborn§   |      |             |             |
|------------|------|-------------|-------------|
| Brain      | 4.0  | 2.1 (80%)   | 16.7 (20%)  |
| Heart Wall | 0.58 | 1.5 (94%)   | ∞ (6%)      |
| Kidney     | 1.2  | 1.8 (75%)   | 21.5 (25%)  |
| Liver      | 4.7  | 4.4 (86%)   | 34.2 (14%)  |
| Lung       | 1.3  | 1.7 (86%)   | 32.2 (14%)  |
| Bone       | 11.8 | 32.3 (100%) |             |
| Spleen     | 0.2  | 2.4 (71%)   | 34.3 (29%)  |
| Remainder† | 76.7 | 8.1 (94.5%) | 37.5 (4.0%) |
|            |      |             | 535 (1.5%)† |

Human retention of <sup>178</sup>Ta assuming uniform blood pool distribution and excretion via the urine

|       |       |             |
|-------|-------|-------------|
| Blood | 100.0 | 1.46 (100%) |
|-------|-------|-------------|

\* Also shown are the two biologic half-lives and percent contributions for each organ obtained by double exponential fitting.

† Adult bladder voiding interval 4.8 hr.

‡ Human whole-body retention data (JNM 24(5):P122, 1983).

§ Newborn bladder voiding interval 1.0 hr.

† Triple exponential fit to whole-body retention data.

radioisotopic purity. Sterility was maintained for the full 30 days of use of each generator in this study.

### Radiation Dosimetry

Utilization of <sup>178</sup>Ta provides greatly reduced patient dosimetry in comparison with <sup>99m</sup>Tc. From Table 5, in adults, whole-body dose is reduced by a factor of 20 relative to <sup>99m</sup>Tc (pertechnetate) while critical organ dose is lowered by a factor of 21. This makes it possible to use high injected activity levels in any given procedure and multiple serial assessment in any given patient. In neonates and small children, <sup>178</sup>Ta provides an agent which can be safely utilized at high dose levels. From Table 6, whole-body dose is reduced by a factor of 19 and critical organ dose by a factor of 50. For example, an injection of 150 mCi of <sup>178</sup>Ta results in the same critical organ dose (11.7 Rems) as the minimum 3 mCi

**TABLE 5**  
Dose Estimates for the Human Adult for <sup>178</sup>W and <sup>178</sup>Ta Compared with <sup>99m</sup>Tc

| Organ                 | <sup>178</sup> W* |          | <sup>178</sup> Ta† |          | <sup>99m</sup> Tc† |          |
|-----------------------|-------------------|----------|--------------------|----------|--------------------|----------|
|                       | μGy/MBq           | mrad/mCi | μGy/MBq            | mrad/mCi | μGy/MBq            | mrad/mCi |
| Bladder wall          | 270               | 990‡     | 1.60               | 6.00‡    | 23                 | 85       |
| Blood                 | —                 | —        | 0.81               | 3.0      | —                  | —        |
| Heart wall            | 7.2               | 27       | —                  | —        | —                  | —        |
| Small intestine       | 17                | 63       | —                  | —        | —                  | —        |
| Upper large intestine | 33                | 120      | —                  | —        | 33                 | 120      |
| Lower large intestine | 76                | 280      | —                  | —        | 30                 | 110      |
| Kidneys               | 24                | 88       | 0.14               | 0.52     | —                  | —        |
| Liver                 | 20                | 74       | 0.14               | 0.54     | —                  | —        |
| Lungs                 | 6.3               | 23       | 0.13               | 0.49     | —                  | —        |
| Ovaries               | 17                | 64       | 0.18               | 0.66     | 8.1                | 30       |
| Red marrow            | 30                | 110      | 0.21               | 0.76     | 4.6                | 17       |
| Skeleton              | 38                | 140      | 0.18               | 0.68     | —                  | —        |
| Spleen                | 8.8               | 32       | —                  | —        | —                  | —        |
| Stomach wall          | —                 | —        | —                  | —        | 14                 | 51       |
| Testes                | 11                | 39       | 0.15               | 0.56     | 2.4                | 9        |
| Thyroid               | —                 | —        | —                  | —        | 35                 | 130‡     |
| Total body            | 13                | 48       | 0.14               | 0.53     | 3.0                | 11       |

\* Intravenous injection of disodium phosphate buffered generator eluate.

† Intravenous injection of <sup>99m</sup>Tc as sodium pertechnetate.

‡ Critical organ.

<sup>99m</sup>Tc injection required for an effective first-pass procedure with [<sup>99m</sup>Tc]pertechnetate.

As a result of the low generator breakthrough performance and excretion characteristics of <sup>178</sup>W, the contribution of <sup>178</sup>W breakthrough to patient dose is negligible. With an average <sup>178</sup>W breakthrough level of 0.001%, <sup>178</sup>W contributes <0.2% of the whole-body dose in both adults and neonates.

#### First-Pass Radionuclide Angiography with the Multiwire Gamma Camera

As a result of the much higher injected activity levels made possible by <sup>178</sup>Ta, considerably improved first-pass radionuclide angiography is possible with a fast imaging device. The MWGC offers an ideal device for such imaging. An x-ray detection efficiency of ~50%

**TABLE 6**  
Dose Estimates for the Human Neonate for <sup>178</sup>W and <sup>178</sup>Ta Compared with <sup>99m</sup>Tc

| Organ                 | <sup>178</sup> W* |          | <sup>178</sup> Ta† |          | <sup>99m</sup> Tc† |          |
|-----------------------|-------------------|----------|--------------------|----------|--------------------|----------|
|                       | μGy/MBq           | mrad/mCi | μGy/MBq            | mrad/mCi | μGy/MBq            | mrad/mCi |
| Bladder wall          | 750               | 2,800    | 21.0               | 78.0‡    | 270                | 1,000    |
| Blood                 | —                 | —        | 13.0               | 48.0     | —                  | —        |
| Brain                 | 55                | 200      | —                  | —        | —                  | —        |
| Heart wall            | 240               | 900      | —                  | —        | —                  | —        |
| Upper large intestine | —                 | —        | —                  | —        | 24.5               | 910      |
| Lower large intestine | —                 | —        | —                  | —        | 22.5               | 830      |
| Kidneys               | 190               | 690      | 2.0                | 7.4      | —                  | —        |
| Liver                 | 180               | 660      | 2.0                | 7.4      | 11.4               | 420      |
| Lungs                 | 110               | 410      | 1.9                | 7.0      | —                  | —        |
| Ovaries               | 160               | 590      | 2.4                | 8.9      | 46                 | 170      |
| Red marrow            | 340               | 1,300    | 2.4                | 8.7      | —                  | —        |
| Skeleton              | 910               | 3,400‡   | 2.4                | 9.0      | —                  | —        |
| Spleen                | 150               | 560      | —                  | —        | —                  | —        |
| Stomach wall          | —                 | —        | —                  | —        | 1,050              | 3,900‡   |
| Testes                | 130               | 500      | 2.2                | 8.0      | 16.2               | 60       |
| Thyroid               | —                 | —        | —                  | —        | 324                | 1,200    |
| Total body            | 170               | 620      | 2.0                | 7.3      | 37.8               | 140      |

\* Intravenous injection of disodium phosphate buffered eluate.

† Intravenous injection of sodium pertechnetate <sup>99m</sup>Tc.

‡ Critical organ.

can be easily obtained and the thin Xe gas medium ( $\approx 0.1 \text{ g/cm}^2$ ) makes it almost transparent to the high-energy, gamma rays of  $^{178}\text{Ta}$ , which pose a significant problem for the NaI detectors (19). The gaseous detector is also very fast, providing a count rate close to one million counts per second. The ability to use high doses and the high count rate of the camera should significantly improve the first-pass technique. The primary limitation of this technique is the poor count-statistics achieved with the NaI gamma camera. With enhanced statistics, first-pass radionuclide angiography has the potential to provide an unequalled means to quantify regional ventricular function since it provides an isolated view of both the right and the left ventricles without interference from adjacent structures. With present NaI technology, acceptable global measurements can be obtained but the count statistics available within small areas of the ventricular image are less than optimal for accurate determination of regional functional parameters. Accurate measurement of regional ejection fraction and ejection and filling rates should be of great value in assessment of coronary disease which is inherently a regional disease. First-pass studies should be possible even in neonatal subjects through the use of pin hole collimation. With  $^{178}\text{Ta}$  activity up to 100 mCi, measurement of right and left ventricle ejection fractions, ejection rates, filling rates and related parameters should be possible.

This improved  $^{178}\text{W}/^{178}\text{Ta}$  generator has significant practical advantages over other generators in nuclear medicine. The long  $^{178}\text{W}$  half-life provides considerable economic advantages over systems such as  $^{195\text{m}}\text{Hg}/^{195\text{m}}\text{Au}$  whose 41.5 hr  $^{195\text{m}}\text{Hg}$  half-life limits useful clinical life to at most a few days. Although the short  $^{178}\text{Ta}$  half-life (39 times shorter than  $^{99\text{m}}\text{Tc}$ ) provides significantly lowered patient dosimetry, the shelf life is long enough to allow many procedures to be done with one generator over several weeks. In addition, the blood-pool labeling characteristics are suitable for multiple gated cardiac studies. Furthermore, lung and liver labeling have been demonstrated (20). Such labeling procedures are very difficult or impossible with systems such as  $^{191}\text{Os}/^{191\text{m}}\text{Ir}$ ,  $^{195}\text{Hg}/^{195\text{m}}\text{Au}$ ,  $^{82}\text{Sr}/^{82}\text{Rb}$ , due to the very short half-life of the injected isotope. Much larger activity levels of  $^{178}\text{Ta}$  relative to  $^{99\text{m}}\text{Tc}$  can be used in these labeling applications, lowering acquisition time and improving image statistics while still providing reduced patient dosimetry.

#### Economic Considerations

The economics of the  $^{178}\text{W}/^{178}\text{Ta}$  generator are attractive even when compared to the low cost  $^{99\text{m}}\text{Mo}/^{99\text{m}}\text{Tc}$ . With internal water-cooled cyclotron targetry, beam currents of 200 to 300  $\mu\text{A}$  have been achieved at 40 MeV at the University of Texas Health Sciences Center Cyclotron. At such currents, production of 100

mCi of  $^{178}\text{W}$  requires significantly less than one hour of cyclotron time. This level of  $^{178}\text{W}$  provides a generator with an initial yield of 60 mCi and a yield of 20 mCi after three weeks of use. Since the utilization time of the  $^{178}\text{Ta}$  generator is three times that of a  $^{99\text{m}}\text{Tc}$  generator, the cost of the system would likely be competitive. Production costs are, of course, higher but this may be more than offset by a factor of three reduction in materials, labor, and shipping costs.

#### REFERENCES

1. Lacy JL, LeBlanc AD, Babich JW, et al. A gamma camera for medical applications using a multiwire proportional counter. *J Nucl Med* 1984; 256:1003-1012.
2. Lacy JL, Verani MS, Ball ME, et al. First-pass radionuclide angiography using a multiwire gamma camera and tantalum-178. *J Nucl Med* 1988; 29:293-301.
3. Neirinckx RD, Jones AG, Davis MA, et al. Tantalum-178—a short lived nuclide for nuclear medicine: development of a potential generator system. *J Nucl Med* 1978; 19:514-519.
4. Neirinckx RD, Trumper J, LeBlanc A, Johnson PC. Radionuclide generators. Evaluation of adsorbents for the Ta-178 generator. ACS Symposium Series, 1983: 151-167.
5. Recommendations of the International Commission on Radiological Protection. In: *Annals of the ICRP; ICRP Publication*, Vol. 38. New York: Pergamon Press 1983: 11-13, 804-805, 827.
6. Holman BL, Harris GL, Neirinckx RD. Tantalum-178—a short lived nuclide for nuclear medicine: production of the parent. *J Nucl Med* 1978; 19:510-513.
7. Ion Exchange Manual. Richmond, California: Bio-Rad Laboratories: 14, 1982.
8. Snyder W, Ford M, Warner G. Estimates of specific absorbed fractions from photon sources uniformly distributed in varying organs of a heterogeneous phantom. MIRD Pamphlet No. 5, Revised. New York: The Society of Nuclear Medicine, 1978.
9. Cristy M, Eckerman K. Specific absorbed fractions of energy at various ages from internal photon sources. Oak Ridge, TN, Part I ORNL/TM-8381, 1987.
10. Babich JW, LeBlanc AD, Lacy JL, et al. Biological fate of tungsten-178 and tantalum-178 [Abstract]. *J Nucl Med* 1983; 24:P122.
11. Zimmerman RE, Holman BL, Neirinckx RD. Dosimetry of tantalum-178 and tungsten-178 in adults and children [Abstract]. *J Nucl Med* 1986; 27:P541.
12. Cloutier R, Snyder W, eds. Medical radionuclides: radiation dose and effects. AEC Symposium Series 20, Conf-691212, Oak Ridge, TN, 1970.
13. Loevinger R, Berman M. A revised schema for calculating the absorbed dose from biologically distributed radionuclides. MIRD Pamphlet No. 1, Revised. New York: The Society of Nuclear Medicine, 1976.
14. Cloutier R, Smith S, Watson S, et al. Dose to the fetus from radionuclides in the bladder. *Health Phys* 1973; 25:147-161.
15. Cloutier R, Watson S, Rohrer R, et al. Calculating the radiation dose to the organ. *J Nucl Med* 1973; 14:53-55.

16. Lathrop K, Atkins H, Berman M, et al. Summary of cumulative radiation dose estimated for normal human from  $^{99m}\text{Tc}$  as sodium pertechnetate. MIRDOse Estimate Report #8. *J Nucl Med* 1976; 17:74-77.
17. Cochran KW, Doull J, Mazor M, et al. Acute toxicity of zirconium, columbium, strontium, lanthanum, cesium, tantalum, and yttrium. *Archs Ind Hyg Occup Med* 1950; 1:637-650.
18. Dechezlepretre PS, Cheymol RPJ. Toxicités comparées de la triméthylamine (TMA), de son oxyde le triméthylaminoxyde (TMAO), et de leur association. *Medicina et Pharmacologia Experimentalis* 1967; 16:529-535.
19. LeBlanc AD, Lacy JL, Johnson PC, et al. Tantalum-178 count-rate limitations of Anger and multicrystal cameras. *Radiology* 1983; 146:242-243.
20. Neirinckx RD, Holman BL, Davis MA. Tantalum-178 radiopharmaceuticals for lung and liver imaging. In: Radiopharmaceuticals II: Proceedings of the 2nd international symposium on radiopharmaceuticals, Seattle, Washington: New York Society of Nuclear Medicine, Inc., 1979: 801-809.